

Roughness with a finite correlation length in a microtrap

Muzhi Wu,¹ Xiaoji Zhou,^{1,*} W. M. Liu,² and Xuzong Chen¹

¹*School of Electronics Engineering & Computer Science, Peking University, Beijing 100871, People's Republic of China*

²*Institute of Physics, Chinese Academy of Sciences, Beijing 100080, People's Republic of China*

(Received 1 December 2009; published 29 March 2010)

We analyze the effects of roughness in the magnitude of the magnetic field produced by a current carrying microwire, which is caused by the geometric fluctuation of the edge of the wire. The relation between the fluctuation of the trapping potential and the height the atom trap lies above the wire is very well consistent with the experimental data when the colored noise with a finite correlation length is considered. On this basis, we generate the random potential and get the density distribution of the Bose-Einstein condensate (BEC) atoms by solving the Gross-Pitaevskii equation, which coincides well with the experimental image, especially in the number of fragmentations. The results help us further understand the nature of the fluctuation and predict its possible application in the precise measurement.

DOI: [10.1103/PhysRevA.81.033625](https://doi.org/10.1103/PhysRevA.81.033625)

PACS number(s): 03.75.Be, 07.55.Ge, 37.10.Gh

I. INTRODUCTION

Trapping and manipulating ultracold atoms and Bose-Einstein condensates (BEC) in a magnetic potential produced by a micro atom chip has attracted more attention recently because it is easy to perform coherent manipulation, transport, and interferometry on a chip [1,2] where the condensate is very close to the surface of the wire. It is possible to bring miniaturization into the application of the BEC [3]. The trapping frequencies in the radial direction are normally several kHz and a few Hz in the axial direction. Hence the aspect ratio is so high that the size of the BEC is several mm in the axial direction; the spatial effects on the condensate will be obvious. However, for the small-scale magnetic field of atom traps produced by micro fabricated current carrying wires, an unexpected problem in these chips was their small fluctuation in the magnetic field, which introduces a random potential along the trap. Such a fluctuation in the potential will cause fragmentation of the atom clouds [2,4]. The effects of the random potential have been studied theoretically [5,6], where the randomness in the magnetic field is due to the geometric fluctuation of the wire surface and the strength of the disorder field shows a $d^{-5/2}$ relation with the height d that the atoms lie above the wire when assuming the correlation of the wire edge is the white-noise correlation. It is not coincidental to the experimentally observed $d^{-2.2}$ relation [7].

The deviation in the theoretical calculations [5,6] from the experiment is caused by the white-noise approximation made, which does not meet the actual situation that the system's fluctuation cannot be the ideal white noise [8,9]. In this article we elucidate the nature of the random potential, indicating the relation between the strength of the potential and the height of the BEC atoms. Different from the white-noise assumption, we consider a more general correlation form—the colored-noise correlation $R(r) = \sigma^2 e^{-|r|/\xi}$, with ξ the correlation length of the system. Here we borrow the notion “colored noise” from the theory for time-domain noise analysis to deal with the case of spatial roughness [10]. Our theory shows that the power index α in the disorder potential $u_s = Cd^{-\alpha}$ is relevant to the

system's intrinsic correlation length ξ . This means that, by measuring the dependence factor α , the correlation length of the current carrying wire can be known. As we point out in the experiment [7], $\alpha = 2.2$ because $\xi = 75 \mu\text{m}$. Consequently, the correlation function for the random potential is calculated.

With the random potential we solve the Gross-Pitaevskii equation, depict the density profile of the captured BEC atoms, and compare it with that of the white-noise case. The desired random potential is generated using a selected aperture function derived from the correlation function. The number of fragmentations has a better agreement with the experiment than previous calculations. This work is meaningful in the simulation of the transport process. It predicts as well a criterion for judging the quality of the wire used for cold-atom manipulation, which might be highly applicable in the precise measurement.

II. THE STRENGTH OF THE DISORDER POTENTIAL

A typical setup of a magnetic microtrap is shown in Fig. 1. The current I_0 flowing in a micro-fabricated copper conductor in the z direction and a bias field B_{bias} in the y direction form a magnetic trap for atoms. The distance d from the surface of the current carrying wire to the center of the trapping potential is controlled by the bias field and the current $d = \mu_0 I_0 / 2\pi B_{\text{bias}}$.

The random potential is brought about by the roughness in the magnetic trap for the BEC atoms lying above the wire surface about $100 \sim 200 \mu\text{m}$. What we are interested in is the z direction of the random magnetic field B_z , which connects with the y component of the current. In experiments [7,11], the wire normally is a thin electroplated Au layer of a few μm thick. The surface of the wire can be made very flat technically with the electroplating method. So the main contribution of the random field arises from the side of the wire.

The distortion of the side edge of the wire curves the current flow. The potential roughness in the magnetic microtrap is induced by this abnormal current. To compute the fluctuation without loss of generality, we make the following assumptions. First, the current I_0 remains constant on the edge of the wire; the amplitude J_0 of the current density \vec{j} is then constant as well. Second, the resistivity remains unchanged along the

*xjzhou@pku.edu.cn

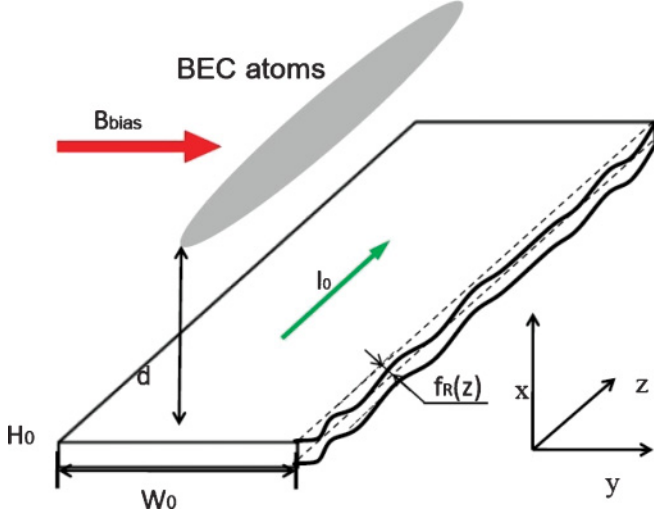


FIG. 1. (Color online) A typical atom chip for the BEC. A constant current I_0 flows in the z direction of the wire with H_0 high and W_0 wide. The BEC atoms lie above the wire at the height of d . A bias magnetic field B_{bias} in the longitudinal direction produces a local minimum. $f_R(z)$ is the deviation of the edge from its ideal position.

current carrying wire. Third, the deviation of the edge from its ideal position (both left and right) $f_{L/R}$ is trivial compared with the width of the wire W_0 , $f_{L/R} \ll W_0$. Considering symmetry, only $f(z) \equiv \frac{1}{2}[f_L(z) + f_R(z)]$ contributes notably to the fluctuation and $f^- = \frac{1}{2}(f_L - f_R)$ is neglected.

If we ignore the change in the module of the current density vector, then we consider the effects due to the alteration of the direction of \vec{j} . The z component of \vec{B} (i.e., B_z) is directly relevant to the y component of the current density. In the yz plane the current density satisfies the charge conservation condition $\frac{\partial j_y}{\partial y} + \frac{\partial j_z}{\partial z} = 0$. Under such assumptions, we introduce an auxiliary scalar potential G , so that $j_y = J_0 \frac{\partial G}{\partial z}$ and $j_z = -J_0 \frac{\partial G}{\partial y}$. The function G satisfies the Laplace equation in the interior of the wire $\nabla^2 G = 0$. Using separation of variables, we get the Fourier component of $f(z)$, which brings a transverse current density [5]

$$j_y \propto J_0 \frac{\partial}{\partial z} \int_{-\infty}^{\infty} \frac{e^{ikz} dk}{\sinh(kW_0)} \cosh(ky) \sinh(kW_0/2) F_f, \quad (1)$$

where F_f is the inverse Fourier transform of $f(z)$, $F_f = \frac{1}{2} \int_{-\infty}^{\infty} dz e^{ikz} f(z)$ and k is the wave vector in the frequency domain.

Therefore the disorder magnetic field can be derived from the Biot-Savart law

$$\vec{B}(\vec{r}) = \frac{\mu_0}{4\pi} \int d^3\vec{r}' \frac{\vec{j} \times \vec{r}}{r^3}. \quad (2)$$

The random potential $U(z)$ is given by $U(z) = -\mu_B B_z$. So the strength of U induced by the roughness in the magnetic microtrap can be measured by the value at the zero point of the potential's autocorrelation function $g(r)$ with $r = z - z'$,

$$g(r) = \langle \delta U(z) \delta U(z') \rangle, \quad (3)$$

where $\langle \dots \rangle$ denotes the ensemble average. And the Fourier transform of $g(r)$ (i.e., the power spectral density of the random

potential) is

$$S(k) = \int dr e^{ikr} g(r). \quad (4)$$

As the wire is electroplated with a thin layer of Au [11], it is acceptable to assume $H_0 \ll d$ and ignore the thickness of the line. We substitute the dimensionless variable $\beta = kd$ for k and obtain

$$S(\beta) = Ad^{-4} \beta^4 P(\beta), \quad (5)$$

with

$$P(\beta) = \frac{2 \sinh(\beta W_0/2d)}{\sinh(\beta W_0/d) (\beta W_0/d)} \sum_{n=0}^{\infty} \frac{(-1)^n}{n! (2y)^n} K_{n+1}(y) \times \gamma \left(2n+1, -\frac{\beta W_0}{2d}, \frac{\beta W_0}{2d} \right) F(\beta/d), \quad (6)$$

where A is a constant, $F(k) = \int d(z-z') e^{-ik(z-z')} \langle f(z) f(z') \rangle$, $K_n(x)$ is the Bessel function of the second kind, and $\gamma(n, x_1, x_2)$ is the incomplete gamma function $\gamma(n, x_1, x_2) = \int_{x_1}^{x_2} dx x^{n-1} e^{-x}$. We then compute the inverse Fourier transform and get the disorder potential u_s^2

$$g(z) = \mathcal{F}^{-1}[S(\beta)] = \frac{1}{d^5} \int_{-\infty}^{\infty} d\beta e^{ik(z-z')} S(\beta), \quad (7)$$

$$u_s^2 = g(0) \sim d^{-5} \int_{-\infty}^{\infty} dk F(k). \quad (8)$$

When the correlation of the wire-edge fluctuation is a white-noise form, $\langle f(z) f(z') \rangle$ is a δ function and $F(k)$ in Eq. (8) is a constant, we have $u_s^2 \sim d^{-5/2}$, which is the same in [5]. The white-noise condition when the edge of the wire is totally not correlated is the simplified case, it limits the supremum of the system fluctuation. In the following we discuss the colored-noise model with a finite correlation length.

III. DEPENDENCE BETWEEN POTENTIAL AND HEIGHT FOR A FINITE CORRELATION LENGTH

The fluctuation $f(z)$ is described as a colored-noise model. The function $f(z)$ is a Gaussian random variable with zero mean $\langle f(z) \rangle = 0$ and variance [8,9]

$$\langle f(z) f(z') \rangle = \sigma^2 e^{-|r|/\xi}. \quad (9)$$

The colored noise given by Eq. (9) is parameterized by three key factors, the distance along the wire $r = z - z'$, the characteristic correlation length ξ , and the noise strength σ . When $\xi \rightarrow 0$, it degenerates into the white-noise correlation form $\langle f(z) f(z') \rangle = \delta(z - z')$, which is the ideal situation of the roughness [5,6]. When $\xi \rightarrow \infty$, the surface of the wire becomes totally correlated, implying a perfect smooth surface, which is the ideal case of the wire. The power spectrum of Eq. (9) for the wire edge is

$$F(k) = \frac{2\xi}{1 + \xi^2 k^2}. \quad (10)$$

When it comes to our model, the wire edge has an intrinsic randomness, the power spectral density of which, described in Eq. (10), is moderate in comparison. The power spectral

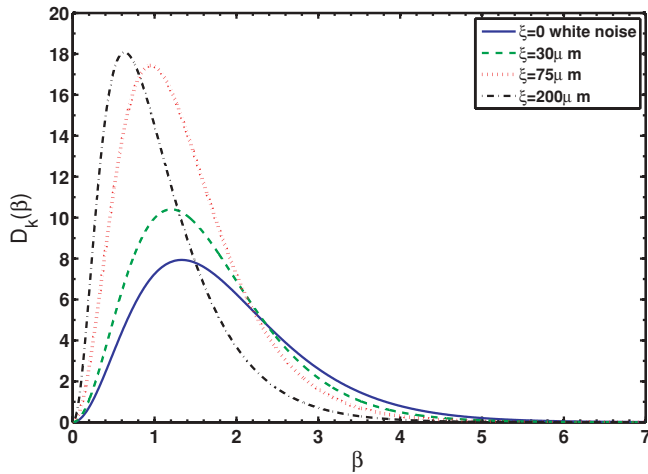


FIG. 2. (Color online) The power spectral function of potential $S(\beta)$ for the different correlation length of the disorder potential. The solid line is for white noise with $\xi = 0 \mu\text{m}$. Others are for the case of colored noise. The dashed line with $\xi = 30 \mu\text{m}$, the dotted line $\xi = 75 \mu\text{m}$, and the dash-dotted line $\xi = 200 \mu\text{m}$.

density of potential $S(\beta)$ for different correlation lengths is shown in Fig. 2. In the white-noise correlation $\xi = 0 \mu\text{m}$, the curve peaks at $\beta = 1.3$. If we choose the typical correlation length $\xi = 75 \mu\text{m}$ [7], the curve peaks at $\beta = 1.1$. From Fig. 2, we know the power spectral density peaks at a smaller value β with the increasing ξ . This means wave vector k decreases and the periodicity weakens for the fluctuation at a certain d . The height of the peak goes up as the correlation length increases, which shows qualitatively that the wire edge becomes smooth so the frequency region is smaller for the disorder potential.

To clarify the effect of the wire width W_0 , we plot the relation between the random potential u_s and the ratio d/W_0 in logarithmic coordinates in Fig. 3. To express it clearly, we can divide the figure into three regions. For distance d varying from 0 to W_0 , the BEC atoms are very close to the top surface of the wire. The relation between the random potential and the ratio

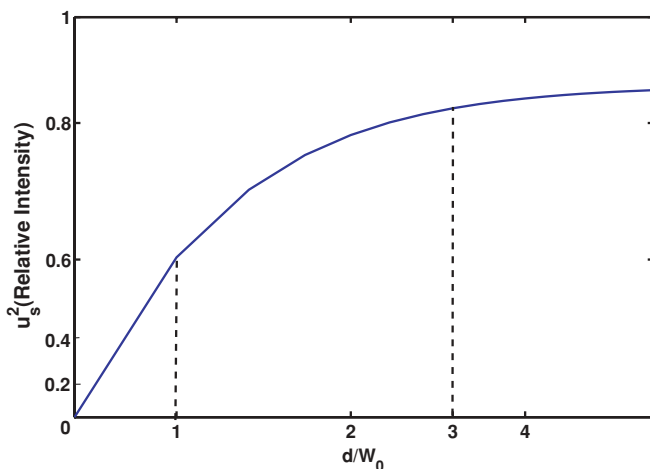


FIG. 3. (Color online) The scaled power spectral density of the random potential and the dimensionless factor d/W_0 in logarithmic coordinates. In the area of $0 < d/W_0 < 1$ and $d/W_0 > 3$, the curve has a good linear fit.

is a linear dependence, which is the fat-line approximation. When $W_0 < d < 3W_0$, the situation becomes complicated, the rim effect of the wire as well as the orbiting magnetic field combine to present a field that cannot be easily calculated theoretically. For distance d ranging from $3W_0$ to infinity, this is also a linear fit corresponding to the thin-line condition. The BEC atoms are far from the top, so the width of the wire can be neglected and the wire as a whole dominates the field. In common experimental conditions [7,11], the atoms are placed high above the surface of the wire with W_0 neglected. So in the following, during our discussion on the $\alpha \sim \xi$ relation, the parameter d we choose mainly ranges from 100 to 200 μm .

The dependence between the strength of the random potential and d can be assumed as

$$u_s = C(d)d^{-\alpha}. \quad (11)$$

Based on the previous analysis, the distance that the atoms lie above the wire d have a linear fit in the logarithmic coordinates for the thin-line approximation when $d \gg W_0$, so $C(d)$ is a constant describing the amplitude of the random fields and α the power index characterizing the speed the fields decays with d . The strength of the disorder potential drops with the growth of height d .

Using Eqs. (8) and (11), we calculate u_s for different ξ and fit them against d to get α . The relationship between α and ξ is plotted in Fig. 4. We can see the potential roughness decays with the height d in direct relation to α . As the correlation length ξ increases, the index α decreases drastically. When ξ is zero, $\alpha \rightarrow 2.5$, which is coincidental to the white-noise approximation. Provided that the deviation between the data from the experiment and theoretical calculation is mainly caused by the uncertainty of ξ , then in our calculations we elucidate the correlation length of the system (i.e., the fluctuation of the edge of the wire should be a finite number on a large scale). For instance, the correlation length in the experiments [7,11] should be 75 μm , pointed out by our figure as well as further calculations. The power index α is determined as soon as ξ is determined.

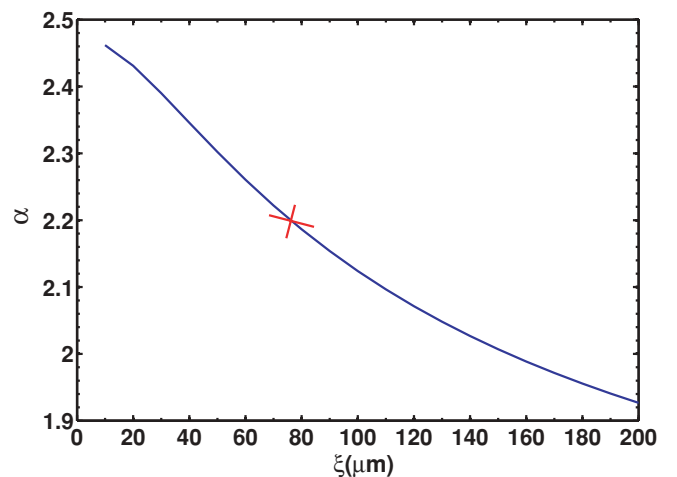


FIG. 4. (Color online) Relationship between the power index α and the correlation length ξ in the case of the thin-line approximation ($d \gg W_0$). The cross point is the typical value $\xi = 75 \mu\text{m}$ and $\alpha = 2.2$.

The strength factor σ^2 in the colored-noise correlation function Eq. (9) only contributes to the constant before the integral in Eq. (7) and is totally not relevant to the shape of the random potential, so it has no effect on the power index α . However, we can see in the following its influence on the density profile is similar to the alteration of the distance d .

IV. THE FORM OF THE ROUGH POTENTIAL AND FLUCTUATIONS OF THE DISTRIBUTION

We then discuss the disturbance of the distribution of BEC atoms caused by the random magnetic fields. The rough potential in the trap can be obtained in the experiments by measuring the density profile of cold-atom clouds via the absorption imaging method. As the BEC atoms expand mainly in the z direction, and are very tight in the other two dimensions, the distribution can be described by the one-dimensional Gross-Pitaevskii equation (GPE) [12]

$$i\hbar \frac{\partial \Psi}{\partial t} = -\frac{\hbar^2}{2m} \nabla^2 \Psi + V(z)\Psi + NU_0|\Psi|^2\Psi. \quad (12)$$

Here, Ψ satisfies the unitary normalization condition, N is the number of BEC atoms, and $U_0 = 4\pi\hbar^2 a/m$ is the intensity of the mean-field interaction. $V(z)$ includes both the harmonic potential and the fluctuated potential as follows [13]

$$V(z) = \frac{1}{2}m\omega_z^2 z^2 + V_d(z). \quad (13)$$

$V_d(z)$ is the random potential induced by the fluctuation and ω_z is the frequency in the z direction. Here we use a method similar to [14] to generate a random potential with the desired correlation function

$$V_d(z) = \mathcal{F}^{-1}[W(k)\mathcal{F}[g(z)]], \quad (14)$$

where $W(k)$ is an appropriate aperture function which can filter out the high and low parts of the signal. With $V_d(z)$ we use a backward Euler finite difference (BEFD) to compute the dynamic evolution of the GPE and finally get the wave function Ψ and the density profile $|\Psi|^2$ [13].

Due to the random potential induced by the fluctuation of the magnetic fields, a series of fragmentations in the condensate density profiles come into being. For different bias field values, the experimental sequence used to produce ultracold atoms in this trap were carried out, corresponding to different distances from the magnetic trap to the top surface of the wire. The strength of the random potential is mainly affected by the value σ^2 in Eq. (9). When the strength is relatively large, the random potential is comparable to the harmonic potential. The fragments present a high peak and the density distribution rises and falls sharply, as shown in Fig. 5.

Figure 6 shows the effect of the disorder strength on the density profile. We focus on the area around the main peak and take out the 1000 μm area. The relative roughness strength in Figs. 6(a) through (d) is 1:2:6:10. From the figure we can see the fragmentation gradually becomes obvious as the strength increases. At the appropriate strength for the random potential, as shown in Fig. 6(c), the density profile basically coincides with the experiment [7]. The amplitude for the fragments are different, with one the highest and the others decreasing accordingly, and the distance between the two peaks in the

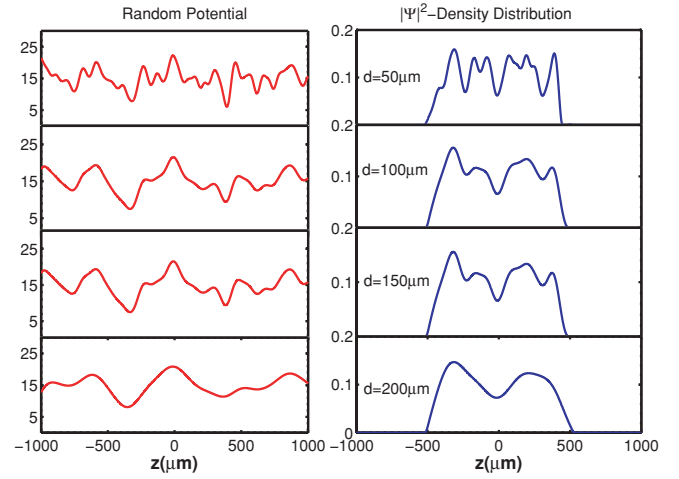


FIG. 5. (Color online) Density profile of the BEC atoms and the random potential at different heights on the case of a large random potential. The left column indicates the random potential at 50, 100, 150, and 200 μm , respectively from top to bottom. The right column is for the normalized distribution $|\Psi|^2$ at the height of 50, 100, 150, and 200 μm from top to bottom. Figures for the $|\Psi|^2$ range are the same from 0 to 0.2. ξ is fixed at 75 μm . [7]

1000 μm area is about 250 μm . The characteristics of the experiment [7] are reflected by our calculations.

First we discuss the effects of height d at a finite correlation length ξ . We can see the dependence between the random potential and the distance in the left column of Fig. 5. It indicates the random potential at 50, 100, 150, and 200 μm . The right column is for the density distribution. Using the equation $u_s^2 = Cd^{-2.2}$ given previously, we can assess the strength of the potential quantitatively. As the distance increases, the roughness of the random potential weakens. Meanwhile the fragmentation phenomenon in the density distribution becomes less obvious.

Then we show the influence of a different correlation length at a fixed height d . Figure 7 demonstrates how the correlation length of the system affects the distribution of BEC atoms.

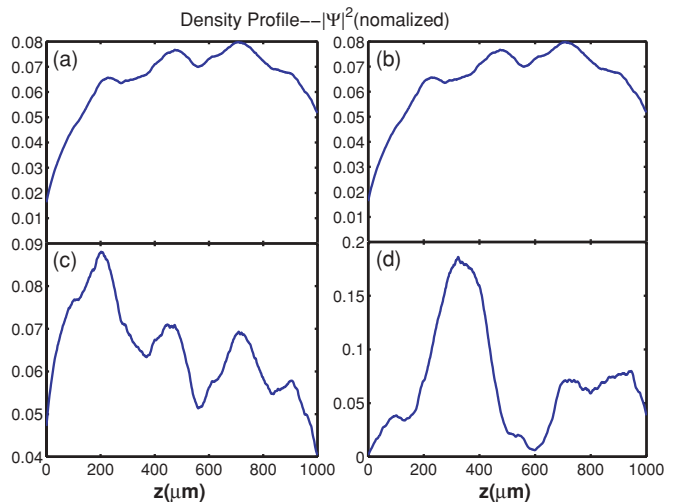


FIG. 6. (Color online) Effect of the disorder strength on the density profile with $\xi = 75 \mu\text{m}$. The relative strength in (a), (b), (c), and (d) is 1:2:6:10.

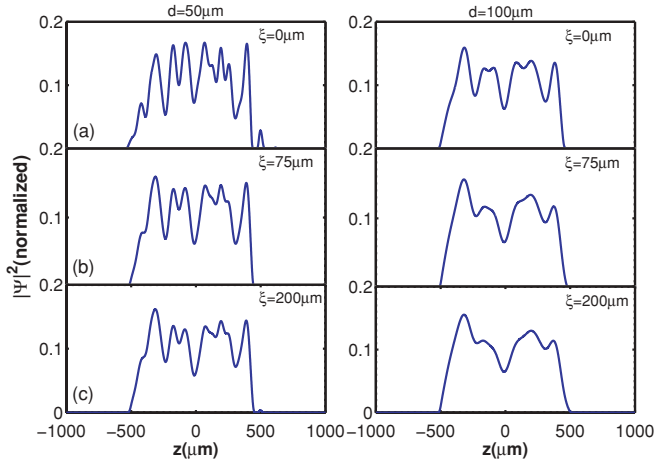


FIG. 7. (Color online) The normalized density profile of the BEC atoms for different correlation lengths. The left column for the height $d = 50 \mu\text{m}$. The right column for $d = 100 \mu\text{m}$. All the figures have the same range for $|\Psi|^2$ from 0 to 0.2. (a) $\xi = 0 \mu\text{m}$, (b) $\xi = 75 \mu\text{m}$, and (c) $\xi = 200 \mu\text{m}$.

The left column is for different correlation lengths 0, 75, and 200 μm at the height $d = 50 \mu\text{m}$, and the right column is for all the same conditions except for $d = 100 \mu\text{m}$. When the system has an intrinsic correlation length, the fragmentation of the density profile is apparently smaller than that of the white noise. In two extreme cases, as $\xi \rightarrow \infty$, the distribution becomes smooth because it is the ideal situation that the current-carrying wire has no fluctuation, while $\xi \rightarrow 0$ is the simple white-noise case and the fluctuation is at its maximum. We are most interested in Fig. 6(c) when $d = 100 \mu\text{m}$ and $\xi = 75 \mu\text{m}$. This set of data is measured in the experiment [7]. The number of the fragmentations, which is about four along the z axis over 1000 μm , is in good agreement with the image derived from the experiment, better than that of the white-noise approximation (about six) which is different from the experimental data.

V. DISCUSSION AND CONCLUSION

According to our analysis, different correlation lengths will lead to different α . As in the experiment [7,11], $\alpha = 2.2$, the

plausible correlation length through our calculations, should be 75 μm , and the density profile we thus get is coincidental with the experiment. The spectral density of the distribution [11] shows that ξ has a very small fluctuation 100 nm, so the features of a system can be considered as a finite correlation length. We also take the width of the wire into account, pointing out exactly how it affects the random potential. Though the real trap is not a thin wire, our model indicates when the height d is relatively large, it is rational to ignore the width of the wire. We then analyze how the strength of the random potential affects the density distribution. The density profile for the appropriate disorder strength in our theoretical picture is in better accordance than the previous white-noise approximation to some extent, which proves our conclusions to be more reasonable. That is to say, by counting the number of fragmentations of the atoms, we can see qualitatively the correlation length of the wire. Furthermore, by measuring the power spectral density of the disorder potential, we can get the correlation length quantitatively.

In summary, we bring forth a more general model to calculate the random potential for the BEC atoms in a current carrying wire. We show that the fluctuation in the potential is caused by the distortion of the wire edge with a fixed correlation length. The correlation length of the specific wire used in the experiment [7] is $\xi = 75 \mu\text{m}$ and the power index in $u_s = Cd^{-\alpha}$ is 2.2. This might be applicable in the precise measurement because of the possible criterion provided for the necessary wire quality to be used for cold-atom manipulation. Besides, by measuring the spectral density of cold-atom distribution and analyzing the deviation in the data we get from theoretical calculations and the experiment, we can get to know the nature of the noise, and apply it in the simulation of the transport process.

ACKNOWLEDGMENTS

X. J. Zhou thanks E. A. Hinds, B. Darquie, and H. T. Yin for their help and discussion. This work is partially supported by the state Key Development Program for Basic Research of China (Grants No. 2005CB724503, No. 2006CB921401, and No. 2006CB921402), and by NSFC (Grants No.10874008 and No. 10934010).

-
- [1] R. Folman, P. Krüger, J. Schmiedmayer, J. Denschlag, and C. Henkel, *Adv. At. Mol. Opt. Phys.* **48**, 263 (2002).
 - [2] J. Fortágh and C. Zimmermann, *Rev. Mod. Phys.* **79**, 235 (2007).
 - [3] W. Hänsel *et al.*, *Nature (London)* **413**, 498 (2001).
 - [4] A. E. Leanhardt, Y. Shin, A. P. Chikkatur, D. Kielpinski, W. Ketterle, and D. E. Pritchard, *Phys. Rev. Lett.* **90**, 100404 (2003).
 - [5] D. W. Wang, M. D. Lukin, and E. Demler, *Phys. Rev. Lett.* **92**, 076802 (2004).
 - [6] T. Schumm, J. Esteve, C. Figl, J. B. Trebbia, C. Aussibal, H. Nguyen, D. Mailly, I. Bouchoule, C. I. Westbrook, and A. Aspect, *Eur. Phys. J. D* **32**, 171 (2005).
 - [7] S. Kraft, A. Gnther, H. Ott, D. Wharam, C. Zimmermann, and J. Fortágh, *J. Phys. B: At. Mol. Opt. Phys.* **35**, L469 (2002).
 - [8] G. Palasantzas, *Phys. Rev. B* **48**, 14472 (1993).
 - [9] Z. Maktadir, B. Darquie, M. Kraft, and E. A. Hinds, *J. Mod. Opt.* **54**, 2149 (2007).
 - [10] X. J. Zhou, *Phys. Rev. A* **80**, 023818 (2009).
 - [11] J. Esteve, C. Aussibal, T. Schumm, C. Figl, D. Mailly, I. Bouchoule, C. I. Westbrook, and A. Aspect, *Phys. Rev. A* **70**, 043629 (2004).
 - [12] F. Dalfovo, S. Giorgini, L. P. Pitaevskii, and S. Stringari, *Rev. Mod. Phys.* **71**, 463 (1999).
 - [13] W. Bao, D. Jaksch, and P. A. Markowich, *J. Comput. Phys.* **187**, 318 (2003).
 - [14] M. Modugno, *Phys. Rev. A* **73**, 013606 (2006).